Risk Layering - A Loss Classification Approach

by

Ali Raisolsadat

Master's research paper requirement
for the degree of
Master of Mathematics (MMath)
in
Centre Computational Mathematics

Waterloo, Ontario, Canada, 2023

Examining Committee Membership

The following served on the Examining Committee for this thesis. The decision of the Examining Committee is by majority vote.

Supervisor(s): Ben Feng
Assistant Professor, Dept. of Statistics and Actuarial Science
University of Waterloo

External Examiner: Chengguo Weng
Professor, Dept. of Statistics and Actuarial Science
University of Waterloo

Author's Declaration

I hereby declare that I am the sole author of this thesis. This is a true copy of the thesis, including any required final revisions, as accepted by my examiners.

I understand that my thesis may be made electronically available to the public.

Abstract

Analysis of historical data spanning the last 60 years reveals a concerning increase in the frequency and severity of extreme catastrophic losses. For instance, an analysis of aggregate loss values from North America in 2005 revealed an estimated loss exceeding the exhaustion threshold, raising concerns about possible insurer bankruptcies. Hurricane Katrina's devastating impact on the United States, with $96.8 billion in property damages, $4.03 billion in crop damages, and 1,451 weather-related fatalities, demonstrated the harsh reality. This alarming trend has given rise to new challenges for insurers and reinsurers, necessitating the development of urgent and innovative loss-layering strategies. To address this pressing issue, we present an innovative loss-layering approach comprising two interwoven steps to offer a compelling solution.

Loss layering offers insurers an integrated framework that allows them to retain specific loss layers while ceding higher layers to reinsurers or solidarity agencies. Our approach then begins with classifying regional losses into "near maximum" and "near minimum" values. Subsequently, the approach allocates the layers, namely the attachment and exhaustion thresholds, by employing non-linear regression for the near maximum and minimum loss values. After the loss-layering, this project provides respective management instruments for each layer to guide insurers in further adaptation planning.

This paper represents pioneering efforts in employing the approximation of the second derivative of a stochastic process for loss-layering, encompassing all losses rather than solely focusing on the tail of the loss distributions. Categorizing regional losses into distinct layers allows insurers to strategically allocate assets, diversify risk, and provide higher and better coverage levels for catastrophe perils, benefiting policyholders. The loss-layering framework paves the way for effective responses to evolving climate patterns and severe weather events, bolstering insurers' adaptation, and extending tailored coverage against catastrophic losses.

Acknowledgements

I would like to thank all the people who made this thesis possible. First and foremost, I like to thank my supervisor, Prof. Ben Feng, who have encouraged, helped and supervised me through my graduate studies and writing this thesis. Without his guidance and supervision, I could have not een able to write this thesis. I would like to thank late Prof. Kai Liu, whom encouraged to pursue my graduate studies at University of Waterloo. Although he is no longer with us, he continues to inspire me by his example and dedication to the students he served over the course of his career. Further, I would like to my family whom supported me through my Masters studies and writing this thesis.

Dedication

To my brother, Amir Hossein. A friend loves at all times, but a brother is born for adversity.

Table of Contents

List of Figures

List of Tables

Chapter 1

Introduction

1.1 Climate Change Crisis in North America

In recent two decades, the global scenario has undergone an extraordinary transformation, marked by a growing and intricate interaction between climate change and the rise of natural disasters [16]. This period is characterized by unparalleled risks associated with these natural hazards, necessitating urgent and effective measures for managing these risks. Discussing these hazards has extended well beyond scientific inquiry, influencing various aspects of society, natural environment, and more importantly economics [32]. The consequences of climate change are evident in the alarming increase in climate-related disasters which are occurring more frequently and with greater severity, emphasizing the importance of strong risk management strategies for proactive approaches to adapt and mitigate the escalating losses caused by these disasters [5][8].

As the third-largest continent on Earth, North America's diverse ecosystems and economies have been increasingly strained by the consequences of a warming planet. One of the most noticeable manifestations of climate change in North America has been the rise in temperatures. Over the past two decades, average temperatures have steadily increased, resulting in more frequent and intense heat waves across the continent. For example, California and Quebec have experienced record-breaking heat, exacerbating the effects and putting vulnerable populations at risk. The prolonged heat waves have strained energy resources, increased demand for cooling, and heightened health risks, emphasizing the urgent need for adaptive measures and sustainable urban planning [9][45][44]. Critical to regulating the global climate system, the Arctic region has undergone rapid and unprecedented changes in the past two decades. The melting of Arctic ice due to rising temperatures has accelerated, leading to rising sea levels that threaten coastal communities across North America. Coastal cities and Canada's Maritime provinces, such as

Prince Edward Island, have witnessed increased flooding and erosion, challenging infrastructure resilience and requiring substantial investments in adaptation strategies [9][46]. The frequency and severity of extreme weather events have become a defining feature of the climate change crisis in North America. Hurricanes, wildfires, droughts, and flooding have struck with alarming regularity, causing devastating economic losses, displacement, and loss of life. The severe hurricanes in the past two decades highlighted the vulnerability of Gulf and Atlantic coastal regions, while unprecedented wildfires in California and Canada's western provinces have destroyed vast swathes of land and led to hazardous air quality levels [62][39][10]. The climate change crisis has environmental ramifications and far-reaching social and economic consequences. Disproportionate impacts on marginalized communities, including Indigenous populations, low-income neighborhoods, and people of color, have highlighted the intersectionality of climate change and social justice. Displacement due to extreme weather events, loss of livelihoods in agriculture and fisheries, and increased healthcare costs due to heat-related illnesses are straining communities and exacerbating existing inequalities [14].

Hence, at this crucial time, there is an immediate requirement to develop and implement policies, representing a pivotal moment in the global efforts to reduce climate-related disaster risks. This urgency is emphasized by the fact that governments, insurers, and financial institutions all bear a substantial burden due to these risks. The effectiveness of adaptation policies in shaping climate disaster risk management is becoming increasingly evident, aligning with fundamental principles of risk governance and building resilience.

1.2 Effect of Climate Change on Insurance Industry

The climate change crisis casts a large shadow over the insurance and reinsurance industries, ushering in unprecedented challenges and complex risk assessment. As the planet's climate evolves, the industry grapples with a shifting landscape of natural disasters, extreme weather events, and mounting financial liabilities. As previously mentioned, climate change has magnified the frequency and severity of natural disasters, propelling the insurance industry into a new territory. The increase in extreme weather events, such as hurricanes, wildfires, floods, and droughts, has led to a surge in insurance claims, placing immense strain on insurers' resources [38]. Furthermore, due to fast changing frequency and severity of weather-related events, insurance industry grapples with the need to recalibrate their risk models. As a result, insurers face the challenge of accurately pricing policies to reflect the new normal of climate-related risks while ensuring their financial sustainability [1].

Amidst these challenges, the insurance industry is responding with innovative strategies to build resilience. Insurance enhances financial resilience and serves as a catalyst for solutions

that promote social and environmental sustainability. Within this context, the insurance industry, encompassing roles as risk managers, carriers, and investors, holds the potential to contribute significantly to sustainable development. As an essential player in risk management, the insurance sector is central in addressing the challenges posed by climate-related disasters. Insurers are exploring advanced technologies such as satellite imagery, aerial drones, and artificial intelligence to assess risks and monitor claims more effectively [2][33].

However, the expanding scope of climate-related risks has led to an uninsurability for the insurance industry. Properties that were once insurable are now facing uncertainty due to heightened exposure to climate hazards. For example, coastal properties prone to storm surges increasingly face challenges in securing affordable coverage. This has significant implications for homeowners, real estate markets, and financial institutions, potentially leading to decreased property values and hindering economic growth [6]. Therefore, a critical evaluation of the industry's approach reveals limitations in coverage for policyholders for various climate and weather-related perils, exposing one of the intricate obstacles within this landscape [43].

1.3 Problem of Classifying Climate and Weather-Related Disasters

As we delve deeper, one of the reasons of this obstacle is the classification of loss, a critical aspect of loss layering. Disaster classification based on severity (incurred loss) categorizes economic losses or damages from particular events or situations [7]. The task of classifying climate and weather-related losses based on severity is not an easy task. If the classification model is poorly constructed, then it can lead to wrong estimations of the potential impact of climate and weather-related disasters, subsequently affecting risk assessment models. Disasters might be underestimated, meaning their potential impact would not be fully recognized, leading to insufficient reserves by the insurer and less coverage for policyholders. Conversely, hazards might be overestimated, resulting in excessive reserves for the insurer and high premiums for policyholders, which subsequently, leads to a low number of insurance policies that offers coverage for climate and weather-related perils.

1.4 Loss Layering in Insurance

Risk or loss layers, or risk-layering, originates from the insurance sector and it is one of important aspects in risk management and governance. It represents a form of non-proportional reinsurance,

a mechanism for transferring risk grounded in loss retention. In this framework, an initial insurer offers coverage up to a predetermined threshold. Beyond this point, a sequence of risk transfers comes into play utilizing the excess of loss strategy. Essentially, the primary insurer retains responsibility for the insured risk until a pre-agreed limit is reached. When this limit is reached, which is often referred to as the attachment threshold, the risk shifts to the following insurance entity in line. This subsequent insurer offers coverage up to another designated limit, known as the the exhaustion threshold. Following this principle, a cascade of excess-of-loss insurance is constructed, with each layer of risk being managed by a separate insurance provider. If losses exceed the exhaustion threshold, it would strain the initial insurer financially or may even lead to insolvency and bankruptcy. This intricate arrangement ultimately facilitates the attainment of substantial insurance coverage for policyholders [21]. Risk layers are applied across various disciplines [40], including agricultural insurance risk management, medical research, social sciences, and environmental science. For instance, medical studies use risk layers to analyze the cumulative effects of risk factors on conditions like diabetes [48], asthma [56], or the effect of gambling on public health [49]. In insurance loss layering is a great tool since it facilitates the expansion of insurers' capacity to underwrite catastrophic risks [21]. For example, loss layering can be extended to encompass both direct and indirect effects and presents a holistic approach to address intricate challenges in disaster risk management and sustainable development [21]. However, there is no systematic approach on how the indirect risks affect the direct risks, and with that, how both the direct and indirect risks affect the loss layering as a whole. Furthermore, loss layering could be used to explore the integration of ambiguity into a risk-layer framework, focusing on risk insurance and mitigation and offering a closed-form solution to assess the implications of ambiguity on the adoption of insurance and risk mitigation using a parametric approach over the tail of loss distribution and using value at risk (VaR) to construct the attachment and exhaustion thresholds [4]. However, the time-dependency of the thresholds are removed due to parametric nature of the approach.

1.5 Classification and Loss Layering Method

Classifying losses is considered the initial step of loss layering, allowing insurers to categorize and understand the various risk components. With a robust classification framework, however, the process of loss layering can become significantly more straightforward, as the lack of clear categorization may hinder the accurate allocation of loss layers. Another major challenge is the limited amount of available data. This makes it difficult to rely solely on the highest and lowest loss values within small incremental periods to create our regression models. To overcome this issue, this paper used a technique called second-order differencing. This method allows us to categorize

data points in a systematic way, removing the need for subjective judgment in selecting the data. Importantly, this approach is supported by mathematical reasoning. Furthermore, catastrophic losses are dynamic and can evolve, especially disasters that are by-products of changes in climate. Therefore, insurers must consistently adjust the loss layers over time. As a result, an appropriate loss classification, with proper mathematical rigor, is an excellent tool for creating effective loss layering strategies. By categorizing various types of catastrophic events based on their historical severity, insurers can set specific thresholds that outline the boundaries between different layers of risk.

Henceforth, to overcome the obstacle of insufficient coverage for policyholders, this paper seeks to construct a model that facilitates determining acceptable loss levels for insurers amidst the ongoing trend of climate-related hazards. The aim is to simplify this complex issue, assisting insurers and policymakers in bolstering their ability to underwrite more policies that will provide coverage for catastrophe perils.

To do so, this paper offers two approaches, where each approach has two interconnected steps for creating loss layers. The first approach uses the aggregated total loss values and the second approach uses the cumulative probabilities of the aggregated total loss values. Both approaches aim to, first, classify loss values into two categories, namely, the "near minimum" and "near maximum" loss values, and then use the two categorizes of losses to construct the attachment and exhaustion thresholds. After setting the thresholds, we can construct the loss layers, namely the low-medium, medium-high and high loss layers.

Initially, we began by applying a second-order difference to the loss values, and with that, we assessed the curvature of this distribution across different time segments. If the sign of the second-order for a time segment was negative, then this segment would be a concave segment. However, if the sign of the second-order difference was positive, then this segment would be convex segment. We classified losses that belonged to a concave segment to be near maximum losses and those that belonged to a convex segment to be near minimum losses.

However, we noticed that the actual loss values can become very large, without a definitive upper boundary. Therefore, we used empirical cumulative probability function (ECDF) to normalize the loss values, with the upper boundary of 1 (since ECDF takes probability values). In similar fashion, we applied a second-order difference to cumulative probabilities across different time segments. This analysis allows us to classify the cumulative probabilities into distinct near maximum and near minimum categories, which are then mapped back to their corresponding actual loss values. We can accomplish this task, as there is a one-to-one correspondence between the loss and the empirical cumulative probability values, and since there this is the case, we can use the same classification of probabilities for the losses.

This classification process is the foundation for establishing a time-dependent framework

(thresholds) that effectively partitions the loss spectrum into two discernible categories. Following this classification, we use a combination of log-transformed losses within each designated category and a linear regression approach to establish the two layers. The initial layer, constructed through the regression method by calculating the average (expected) value of near minimum loss values, represented as the attachment threshold, will give the low-medium loss layer. Following that, a similar process was employed to establish the second layer, utilizing regression model on the near maximum loss values to construct the exhaustion threshold, giving us the medium-high loss layer. The losses above the exhaustion threshold will be considered the high loss layer. After constructing the layer, this paper provides a lists of possible financial mechanisms that can help the insurer to properly plan for future drastic natural hazards.

This methodology hopes to surpass the conventional approach by incorporating direct and indirect risks (total losses). By using the second-order difference assessment of curvature to classify loss values, using both the loss and cumulative probability space, this method aptly captures the complex dynamics of loss behavior in simple mathematical formulations. This process enables insurers to tailor their risk allocation and reinsurance structures to match the severity of each classified event, ensuring a robust and adaptable framework for managing catastrophic risks. In essence, the process of classifying losses empowers insurers to make informed decisions when designing their loss layering strategies. This innovative approach, offers a potent solution to enhance global risk management strategies, particularly aligning with goals such as Sustainable Development and Disaster Risk Reduction frameworks.

1.6 Second-order Difference

In section 1.5, we mentioned utilizing the second-order difference for the classification task. The central second-order difference is a mathematical concept for analyzing time series data. It involves calculating the difference between consecutive data points in a time series and then computing the difference again on the resulting sequence of differences. This technique is beneficial for identifying patterns, trends, or changes in the rate of change within a time series. It can help uncover more subtle insights into the underlying information of the data and assist in various applications, such as detecting turning points or fluctuations in a time-dependent phenomenon. The definition of the central second-order difference for a time-dependent loss vector $\boldsymbol{x}$ is given as following.

Definition 1.6.1 (Second-order Difference of Loss)**.** Let $\{x_t\}$ denote the sequence of loss values at different time points $t = 1, 2, ..., 60$. The central finite difference of the loss at time t, denoted as $\frac{d^2x_t}{dt^2} \approx \hat{x}_t''$, is defined as:

$$\hat{x}_t'' = x_{t+1} - 2x_t + x_{t-1} \tag{1.6.0.1}$$

where x_{t+1} represents the loss at time $t+1$, x_t represents the loss at time t, and x_{t-1} represents the loss at time $t-1$. Evaluating the second-order difference for all loss values through time will give us a vector $\hat{\boldsymbol{x}}''$. In this formula, x_t'' represents the central second-order difference of the vector $\boldsymbol{x}$ at time t. It is calculated by subtracting twice the value of x_t from the sum of its adjacent values x_{t+1} and x_{t-1}. It considers the differences between three consecutive points in the vector, or a segment within a vector, providing insights into the rate of change of the original data [54][58][57].

For the boundaries of the second-order difference, at $t = 1$, at the initial time index in time, we have

$$\hat{x}_1'' = x_0 - 2x_1 + x_2$$

A reasonable assumption, based on Neumann boundary condition [51] is to let $\hat{x}_1'' = \hat{x}_2''$. Then we will have

$$x_0 = 3x_1 - 3x_2 + x_3$$

Substituting the new term for x_0 into $\hat{x}_1''$ will give us

$$\hat{x}_1'' = x_1 - 2x_2 + x_3$$

which is the *forward difference* scheme.

At $t = 60$, at the initial time index in time, we have

$$\hat{x}_{60}'' = x_{59} - 2x_{60} + x_{61}$$

A reasonable assumption (based on Neumann boundary condition) is to let $\hat{x}_{59}'' = \hat{x}_{60}''$. Then we will have

$$x_{61} = 3x_{60} - 3p_{59} + x_{58}$$

Substituting the new term for x_{61} into $\hat{x}_{60}''$ will give us

$$\hat{x}_{60}'' = x_{60} - 2x_{59} + x_{58}$$

which is the *backward difference* scheme.

This central second-order difference operation helps to capture information about the acceleration or curvature of the time series data. Please see proof of the second-order difference schemes at Appendix A.1.

1.7 Regression Modelling

In Section 1.5, we mentioned utilizing regression modelling for constructing the attachment and exhaustion thresholds. The following is a summary of how these models are constructed, and the full detail of their usage will be shown in the methodology Chapter 2.

1.7.1 Linear Regression

Linear regression is a statistical method used to model the relationship between a dependent variable and one or more independent variables by fitting a linear equation to the observed data. Linear regression aims to find the best-fitting straight line (or hyperplane in higher dimensions) that minimizes the difference between the observed data points and the predicted values given by the linear equation. The fitted line represents the expected value of the dependent variable for a given unit change in the independent variable. Mathematically, for a simple linear regression model with one independent variable x and a dependent variable y, the fitted line can be expressed as

$$\boldsymbol{y} = \beta_0 + \beta_1 \boldsymbol{x} + \epsilon \tag{1.7.1.1}$$

where, $\boldsymbol{y}$ is the target variable (actual value mapped from $\boldsymbol{x}$), $\boldsymbol{x}$ is the independent variable, β_0 is the intercept term, β_1 is the coefficient associated with the independent variable $\boldsymbol{x}$, and ϵ represents the error term which is normally distributed with a mean of 0 and standard deviation σ ($\epsilon \sim Norm(0, \sigma)$). Since the fitted value $\boldsymbol{y}$ includes an error term, then the fitted line equation can be written as

$$\hat{\boldsymbol{y}} = \beta_0 + \beta_1 \boldsymbol{x} \tag{1.7.1.2}$$

where $\hat{\boldsymbol{y}}$ is an approximation of the function $\boldsymbol{y}$. We can further write that

$$E[\boldsymbol{y}|\boldsymbol{x}] = \beta_0 + \beta_1 \boldsymbol{x} \tag{1.7.1.3}$$

since the fitted value represents the expected value of the dependent variable $\boldsymbol{y}$ for a given unit change in the independent variable $\boldsymbol{x}$ [22].

1.7.2 Polynomial Regression

Similarly, the polynomial regression extends linear regression by using higher powers of the independent variable to model complex non-linear relationships. The model equation is

$$\hat{\boldsymbol{y}} = \beta_0 + \beta_1 \boldsymbol{x} + \beta_2 \boldsymbol{x}^2 + \ldots + \beta_n \boldsymbol{x}^n \tag{1.7.2.1}$$

where $\hat{\boldsymbol{y}}$ is the approximation of the target variable, $\boldsymbol{x}$ is the independent variable, n is the degree of the polynomial, $\beta_0, \beta_1, \ldots, \beta_n$ are the coefficients [22].

1.7.3 Linear Regression Models with Logarithmic Transformations

In log-transform of dependent variable regression [22], the dependent variable y is transformed using a logarithmic function before performing regression analysis. The model can be represented as

$$\widehat{\ln \boldsymbol{y}} = \beta_0 + \beta_1 x \boldsymbol{x} \tag{1.7.3.1}$$

where $\widehat{\ln \boldsymbol{y}}$ is the natural logarithm of the approximation of $\boldsymbol{y}$, the target variable. We an use exponential to get $\hat{\boldsymbol{y}}$ as

$$\hat{\boldsymbol{y}} = e^{\beta_0 + \beta_1 \boldsymbol{x}} \tag{1.7.3.2}$$

1.7.4 Solving for Regression Models

Solving regression models involves finding the optimal coefficients, β, that best represent the relationship between variables $\boldsymbol{y}$ and $\boldsymbol{x}$. The least squares method is a central concept aiming to minimize the sum of squared differences between observed and predicted values. This method leads to the formulation of Normal equations, which provide a system of equations to solve for the coefficients directly. To accomplish this task we can use the `lm()` function in `R` software [22].

1.7.5 Goodness of Fit and Significance

The following measures provide valuable insights into the quality, significance, and complexity of regression models, helping researchers choose the most appropriate model for their data [22].

Coefficient of Determination - R^2

R^2 is a statistical measure representing the proportion of the variance in the dependent variable explained by the independent variables in a regression model. It quantifies the model's goodness of fit to the observed data, ranging from $0 - 1$, where higher values indicate a better fit. Mathematically, for linear regression, we can evaluate R^2 as

$$R^2 = \frac{\text{Variation Explained}}{\text{Total Variation}} = \frac{\sum_{i=1}^{n}(y_i - \hat{y}_i)^2}{\sum_{i=1}^{n}(y_i - \overline{\boldsymbol{y}})^2} \tag{1.7.5.1}$$

P-value

The p-value is a measure used to assess the statistical significance of the relationship between independent variables and the dependent variable in a regression model. It indicates the probability of observing the obtained results (or more extreme results) if the null hypothesis is true. A small p-value (typically less than 0.05) suggests the relationship is statistically significant.

Akaike Information Criterion - AIC

AIC is a model selection criterion that balances the goodness of fit of a model with its complexity. It penalizes models with a larger number of parameters to prevent overfitting. AIC aims to find the model that best explains the data while avoiding unnecessary complexity. AIC is given as

$$AIC = -2\log(L) + 2k \tag{1.7.5.2}$$

where L is the likelihood of the model and k is the number of parameters. In the case of AIC, a smaller value is preferred. A lower AIC suggests that the model fits the data well while using fewer parameters, which reduces the risk of overfitting and promotes model simplicity.

Bayesian Information Criterion - BIC

Similar to AIC, BIC is another model selection criterion that penalizes complex models. BIC places a stronger penalty on additional parameters, making it more stringent in model selection. BIC is given as

$$BIC = -2\log(L) + k\log(n) \tag{1.7.5.3}$$

where n is the number of observations. Analogous to AIC, a smaller BIC value is preferred. A smaller BIC indicates that the model fits the data well, balancing goodness of fit and model complexity. However, BIC penalizes model complexity more strongly than AIC, making it more inclined towards simpler models.

1.8 Financial Mechanisms for Loss Layers

Currently, there are strategies available for insurers to prepare for each loss layer. These strategies are more appropriate for the North America region, however, they could be used in other geographical regions.

For the low-medium loss layer (losses until attachment threshold), this paper suggests strategies that mainly focus on investing in structural improvements and increasing financial reserves through premiums and reinvesting of these premiums. However, cost-effective risk reduction techniques become more challenging as loss values escalate to higher layers. Therefore, for the medium-high loss layers, insurers must explore options such as public and donor support or publicly backed insurance (through *solidarity*) or risk transfer mechanisms (through *reinsurance*) [37]. To bolster an insurer's resilience in such scenarios, exploring the various risk financing approaches available is prudent. For example, they can effectively leverage mechanisms like government and humanitarian aid, savings, credit, informal risk sharing, and alternative risk-transfer instruments to finance recovery.

Insurers can implement diverse strategies in the context of high loss layers, including reliance on government support mechanisms like guarantees, bailouts, and contributions from private and public entities. Government backing is a stabilizing force, reinforcing insurers' capacity to manage substantial losses effectively [23][30]. Challenges intensify in small and highly exposed countries as governments encounter post-disaster fiscal constraints, reducing their ability to support private and public insurers to reach their obligations to the policyholders. However, in these circumstances, international assistance emerges as a lifeline from a collective front comprising individuals, non-governmental organizations (NGOs), and governments in the global community [3]. Leveraging government guarantees and bailouts, insurers can address losses exceeding the exhaustion threshold, ensuring financial stability, timely compensation for policyholders, and enhanced resilience, particularly when extraordinary events strain insurers' resources and require supplementary liquidity injection from governments or international assistance. By capitalizing on solidarity and the combined support of government guarantees, bailouts, and donations from organizations, insurers can navigate the challenges inherent in the high loss layer.

To effectively address losses within the medium-high loss layer (between attachment and exhaustion thresholds) through solidarity, insurers are encouraged to (1) leverage emergency relief funds and (2) engage in private-public partnerships to strengthen their capacity to handle losses [37]. These strategic approaches offer valuable resources, financial support, and collaborative frameworks that can enhance insurers' resilience and response capabilities. Emergency relief funds designed explicitly for climate disasters and insurance defaults provide insurers with immediate access to liquidity during times of crisis. These funds are established by governments, international financial institutions, or specialized insurance facilities to ensure the swift provision of financial support.

For example, the Federal Emergency Management Agency (FEMA) administers the National Flood Insurance Program (NFIP), an emergency liquidity fund designated to support policyholders in the United States facing flood-related losses [19]. This program provides emergency funding and liquidity to insurers to ensure the timely payment of flood insurance claims, helping

stabilize the insurance market during climate disaster events. Emergency Liquidity Assistance (ELA) in Canada is another facility that supports financial institutions, including banks, in times of liquidity stress. The ELA program allows eligible financial institutions to borrow funds from the Bank of Canada by pledging collateral, typically government securities or other high-quality assets. Like other financial institutions, insurance companies can access ELA if they meet the eligibility criteria during severe liquidity constraints. However, the specific terms and conditions for insurance companies to access ELA would depend on the circumstances and the assessment of the Bank of Canada [13].

In addition to solidarity and public strategies, insurers are encouraged to leverage traditional reinsurance methods to manage and mitigate risks within the medium-high loss layer. Traditional reinsurance allows insurers to transfer a portion of the risk associated with the medium-high loss layer to reinsurers [27]. This approach provides insurers a safety net and enables them to meet their obligations to policyholders within the medium-high loss layer. In addition to traditional reinsurance, financial reinsurance offers insurers specialized coverage for specific financial risks within the medium-high loss layer. Financial reinsurance differs from traditional reinsurance, focusing on addressing financial risks rather than insurable ones. While traditional reinsurance transfers the risk of potential losses from one insurer to a reinsurer, financial reinsurance goes a step further by providing coverage for specific financial concerns faced by insurers. Financial reinsurance arrangements often involve the transfer of financial exposures such as reserve inadequacy, credit risk, or variations in financial performance [59].

Furthermore, the insurers can utilize non-traditional reinsurance for the medium-high loss layer. An example of non-traditional commercial reinsurance for managing risks within the medium-high loss layer is the utilization of catastrophe bonds. Catastrophe bonds provide insurers with a unique tool where investors assume the financial risks associated with predefined catastrophic events, explicitly targeting the medium-high loss layer. By incorporating catastrophe bonds into their risk management strategy, insurers can effectively transfer and mitigate the financial risks within the medium-high loss layer while leveraging investor participation [11].

Chapter 2

Methodology

2.1 Data Review

The project uses data from the Emergency Events Database (EM-DAT) database, a renowned and widely-used resource for documenting and analyzing global disaster events. EM-DAT, maintained by the Centre for Research on the Epidemiology of Disasters (CRED), compiles comprehensive information on natural and technological disasters worldwide [17][25][50].

On this natural disasters are categorized into six groups (geophysical, meteorological, hydrological, climatological, biological, and extraterrestrial), which cover 15 specific disaster types and over 30 sub-types. There are various sources that contribute to the database, including governments, United Nations agencies (such as UNEP, UNOCHA, WFP, and FAO), non-governmental organizations, research institutions, insurance companies, and media reports. Inclusion criteria for the database involve events with a minimum of ten fatalities, at least one hundred individuals affected, the declaration of a state of emergency, and/or a call for international assistance. Data entries are recorded at the country level, containing attributes such as location, date, casualties (deaths, injuries, and missing persons), displacement (homeless or affected individuals), economic losses (direct and indirect), international aid contributions, and composite indicators. The classification system used in the database is adapted from Integrated Research on Disaster Risk (IRDR) Peril Classifications. The data entry guidelines follow three levels. At Level 1, information about the disaster event includes its group, sub-group, disaster type, sub-type, and sub-sub-type. Moving to Level 2, geographic and temporal details, physical characteristics, and status are provided. This level includes spatial divisions specifying the continent, country, region, latitude/longitude coordinates, International Organization for Standardization (ISO) code, start/end dates, and local time. The physical characteristics encompass the event's origin, as-

sociated disasters, and scale/intensity measured in relevant units (e.g., wildfire area coverage or earthquake magnitude on the Richter scale). Level 3 contains the source of information and a reliability score (ranging from one to five). This level also covers the human impact, including deaths, missing persons, homelessness, injuries, and affected individuals needing immediate assistance. The economic impact details are also part of level 3, such as total estimated damages, reconstruction costs, insured losses, and the overall disaster impact [17][15].

Since this project's scope was to analyze the damages from climate events and catastrophes, then the dataset used in this project focuses specifically on the direct and indirect tangible cost caused by climatological, hydrological, and meteorological events, estimated by EM-DAT database. These events include but are not limited to, various phenomena such as extreme temperatures, storms, floods, landslides, wildfires, glacial lake outbursts, and droughts. Direct tangible costs are expenses incurred directly due to the physical impact of an event, including damages to infrastructure and property such as buildings, vehicles, livestock, and crops. The estimated damages reported in the dataset represent the combined value of all damages and economic losses directly or indirectly linked to the disasters. These estimated damages are inflation-adjusted to provide a more accurate representation of the economic impact of the events over time. The consumer Price Index (CPI) adjustment was employed bt EM-DAT database to adjust estimated losses to the 2021 USD [17].

In short, the data utilized in this study represents the estimated annual total aggregated losses, which aims to capture the direct tangible costs associated with the events under investigation ((see Figure 2.1). This project focuses on estimated damages and losses in North America from 1963 to 2022. Let us review some of the events that have happened during this period.

In August 1992, Hurricane Andrew made landfall in South Florida as a Category 5 hurricane, leaving behind a path of destruction. With winds reaching a ferocious 165 mph, the hurricane resulted in estimated damages of $27.3 billion. The scale of devastation was extensive, with 126,000 single-family houses destroyed, 9,000 mobile homes damaged, and 65 fatalities recorded. The profound impact of Hurricane Andrew led to significant revisions in building codes and disaster preparedness measures in the region, aiming to mitigate future hurricane-related losses [55]. A case study indicated that 78.2% of households with hurricane damage were covered by property insurance, while approximately 6% of insured households received no settlements, likely due to damages falling below their insurance policy deductibles. The average compensation for Miami-Dade County (Florida state) was about $32,000 [52].

Remarkably, seven of the ten most expensive hurricanes in U.S. history occurred within a 14-month period from August 2004 to October 2005. In September 2004, Hurricane Ivan impacted multiple countries in the Caribbean region and made a second landfall in the United States, battering the Gulf Coast as a powerful Category 4 hurricane. On September 16, 2004, Hurricane

Ivan struck the Florida-Alabama coastline with winds exceeding 140 mph, accompanied by torrential rainfall, storm surge, and coastal flooding 10 to 16 feet above normal tide levels. The hurricane caused damage to 75,000 homes and forced 50,000 people to evacuate from Florida's westernmost counties of Escambia and Santa Rosa. The region was declared a federal disaster area, leading the Federal Emergency Management Agency (FEMA) to provide aid through water, ice, and food distribution to assist affected residents. This widespread devastation prompted a reevaluation of hurricane evacuation procedures and emergency response plans in the United States. Following Hurricane Ivan, the National Flood Insurance Program (NFIP) paid $869 million for 9,800 claims in Florida [41]. In August 2005, Hurricane Katrina struck the Gulf Coast, with New Orleans, Louisiana, facing the brunt of its devastating impact. This hurricane was deemed one of the most catastrophic in U.S. history. Private insurers incurred significant losses, with estimates ranging from $40 to $60 billion, making Hurricane Katrina the costliest natural disaster ever recorded in the country, surpassing even the expensive Hurricane Andrew in 1992 [28]. The toll was not merely financial but also human, with 1,392 lives lost. The extensive damage caused by Hurricane Katrina was estimated between $97.4 billion and $145.5 billion, primarily affecting New Orleans and its environs in late August 2005 [29]. The 2005 wildland fire season in Canada, specifically in British Columbia (BC), Ontario (ON), and Québec (QC), has exhibited a level of activity close to the ten-year average. By the end of 2005, Canada had registered a total of 7,438 fires, consuming approximately 1,706,445.49 hectares of land [24]. In the same year, Hurricane Wilma caused at least eight reported deaths in Mexico, resulting in significant insured and total damage estimates. Insured damages in Mexico were estimated to be between $1 to $3 billion, while the total damage reached approximately $2 to $5 billion. The region, particularly the Cancún area, faced extensive structural damage, severe flooding, downed trees and power lines, and a substantial accumulation of debris [12].

In 2021, winter Storm Uri brought unprecedented cold temperatures and heavy snowfall across the southern United States, including Texas. The extreme cold led to power outages, water supply disruptions, and loss of lives, with an estimate economic loss that is estimated to be around $90 billion [42]. Furthermore, a combination of dry conditions and high temperatures fueled widespread wildfires along the West Coast of the United States, particularly in California, Oregon, and Washington. These fires caused an estimated 3,800 civilian deaths, 14,700 civilian injuries, and $15.9 billion in direct property damage [20]. Poor air quality due to smoke mixed with the COVID-19 pandemic has had far-reaching health implications [60].

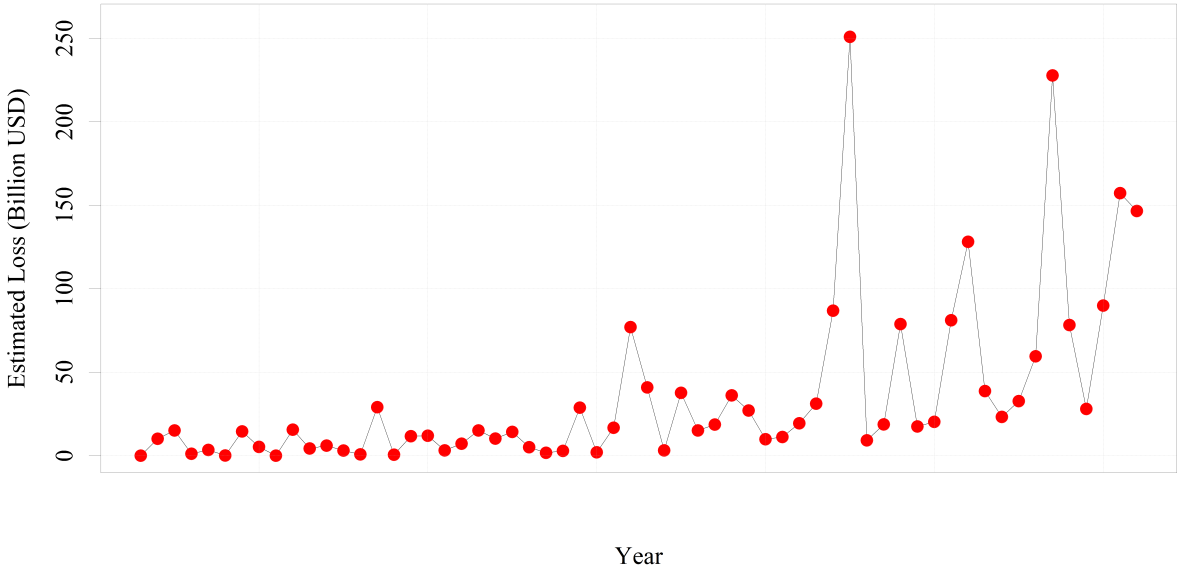

Figure 2.1: Estimated aggregate total losses for Central and North America region from EM-DAT databsase.

2.2 Aggregated Losses - Loss Classification Approach I

To begin the classification task, we utilize the second-order difference over the loss values. We used the second-order difference Definition 1.6.0.1 of Section 1.6.1 for the loss values. The second-order difference in terms of is the rate of change of the rate of change. In other words, it measures how the rate of change of the loss values is itself changing. This concept helps us to make assessment over the curvature loss over 3 time steps (a segment of loss values). Therefore, a positive second-order difference indicates an increasing rate of change loss values, suggesting a potentially reaching a maximum loss value throughout the period of $t+1$, t and $t-1$, giving us a convex segment of loss values. Conversely, a negative second-order difference implies a decreasing rate of change, indicating a potential reaching a minimum loss value throughout the period of $t+1$, t and $t-1$, giving us a concave segment of loss values.

Then we use the concave and convex segments of the aggregate loss to formally define the near maximum and near minimum classification of loss values.

Definition 2.2.1 (Loss classification using the Second-order Difference of Loss)**.** Let $\hat{\boldsymbol{x}}''$ be the discrete values of the second-order difference of the loss space with respect to time. We partition $\boldsymbol{x}$ in two subsets using $\hat{\boldsymbol{x}}''$ as following. The first subset, namely $\boldsymbol{x}^{Nmin}$, represents the concave segments of the loss values, which classifies the near maximum loss values, defined as

$$\boldsymbol{x}_{Nmax} = \{x_t \in \boldsymbol{x} | \text{ the second-order difference is negative at time } t\text{: } \hat{x}_t'' < 0\} \tag{2.2.0.1}$$

The second subset, $\boldsymbol{x}^{Nmin}$ represents the convex segments of the loss values, which classifies the near minimum loss values, defined as

$$\boldsymbol{x}_{Nmin} = \{x_t \in \boldsymbol{x} | \text{ the second-order difference is positive at time } t\text{: } \hat{x}_t'' > 0\} \tag{2.2.0.2}$$

Figure 2.2 illustrates this loss classification using this approach.

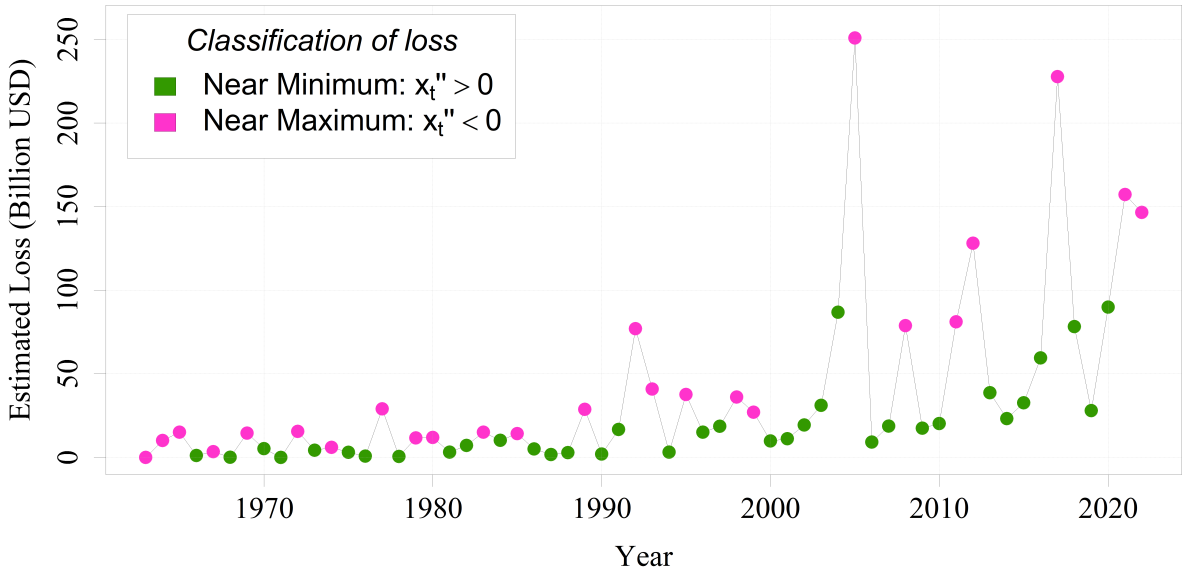

Figure 2.2: Classification of losses using the second-order difference of the loss values.

2.3 Cumulative Probabilities - Loss Classification Approach II

In empirical studies for hazards and catastrophes, the empirical cumulative distribution function (ECDF) are essential tools for analyzing and understanding the frequency and severity of events. Intuitively, the more severe events tend to happen with a smaller probability (less frequently), and the less severe events tend to happen with a larger probability (more frequent). Based on observed data, the empirical cumulative distribution represents the cumulative probability associated with a specific event or hazard. An advantage of using probabilities is that they are bounded between $0 - 1$ (see Figure 2.3), however, there is no specific upper boundary for loss values (see Figure 2.1). We can use this advantage to normalize the loss values before applying similar methodology to classify loss values. We define the ECDF for estimated loss values as following.

Definition 2.3.1 (Empirical Cumulative Distribution Function)**.** Let vector $\boldsymbol{x} = (x_1, x_2, ..., x_t, ..., x_{60})$ represent the aggregated (estimated) loss values for a region. The empirical cumulative function is given as

$$\hat{F}(x) = \frac{1}{60} \sum_{i=1}^{60} \mathbb{1}_{\{x_i \leq x\}} \tag{2.3.0.1}$$

where $\hat{F}(x)$ is an estimation of the real cumulative distribution function $F(x)$ for aggregate losses. Note that the cumulative distribution function is non-decreasing.

Our main objective is the quantify how fast the probabilities are accelerating or decelerating, which in turn provide information about the changes in the rate of change of the loss values. To do so, we need to approximate the second derivative (convexity/concavity) of the probabilities trajectory. We utilize the second-order difference to approximate the second derivative.

Definition 2.3.2 (Second-order Difference of Cumulative Probability Function)**.** Let $\{p_t\}$ denote the sequence of cumulative probabilities at different time points $t = 1, 2, ..., 60$. The central finite difference of the cumulative probability at time t, denoted as $\frac{d^2 p_t}{dt^2} \approx \hat{p}_t''$, is defined as:

$$\hat{p}_t'' = p_{t+1} - 2p_t + p_{t-1} \tag{2.3.0.2}$$

where p_{t+1} represents the cumulative probability at time $t + 1$, p_t represents the cumulative probability at time t, and p_{t-1} represents the cumulative probability at time $t - 1$. Evaluating the second-order difference for cumulative probabilities will give us a vector $\hat{\boldsymbol{p}}''$. The boundaries of the second-order difference can be constructed using the Neumann boundary condition similar to definition 2.2.1.

Similarly, use the concave and convex segments in the cumulative probabilities to classify loss as following.

Definition 2.3.3 (Loss classification using the Second-order Difference of the cumulative Probability)**.** Let $\hat{\boldsymbol{p}}''$ be the discrete values of the second-order difference of the cumulative probability space with respect to time. We partition $\boldsymbol{p}$ in two subsets using $\hat{\boldsymbol{p}}''$ as following. The first subset, namely $\boldsymbol{p}^{CN}$, represents the concave segments of the cumulative probabilities, which is defined as

$$\boldsymbol{p}^{CN} = \{p_t \in \boldsymbol{p} | \text{ the second-order difference is negative at time } t : \hat{p}_t'' < 0\} \tag{2.3.0.3}$$

The second subset, $\boldsymbol{p}^{CX}$ represents the convex segments of the cumulative probabilities, defined as

$$\boldsymbol{p}^{CX} = \{p_t \in \boldsymbol{p} | \text{ the second-order difference is positive at time } t : \hat{p}_t'' > 0\} \tag{2.3.0.4}$$

By using the definition above, namely the two sets $\boldsymbol{p}^{CN}$ and $\boldsymbol{p}^{CX}$, we can classify the near maximum and near minimum losses, by mapping back the these cumulative probabilities back to their corresponding losses. We define group $\boldsymbol{x}_{Nmax}$ of losses that contains the mapped values of elements from $\boldsymbol{p}^{CN}$ to $\boldsymbol{x}$, which are classified as near minimum loss values, as following.

$$\boldsymbol{x}_{Nmax} = \{x_t \in \boldsymbol{x} | \text{ there exists } p_t \in \boldsymbol{p}^{CN} \text{ such that } \hat{F}^{-1}(p_t) = x_t\} \tag{2.3.0.5}$$

Furthermore, we define the $\boldsymbol{x}_{Nmin}$ of losses that contains the mapped values of elements from $\boldsymbol{p}^{CX}$ to $\boldsymbol{x}$, which are classified as near maximum loss values, as following.

$$\boldsymbol{x}_{Nmin} = \{x_t \in \boldsymbol{x} | \text{ there exists } p_t \in \boldsymbol{p}^{CX} \text{ such that } \hat{F}^{-1}(p_t) = x_t\} \tag{2.3.0.6}$$

Figure 2.4 illustrates this loss classification using this approach.

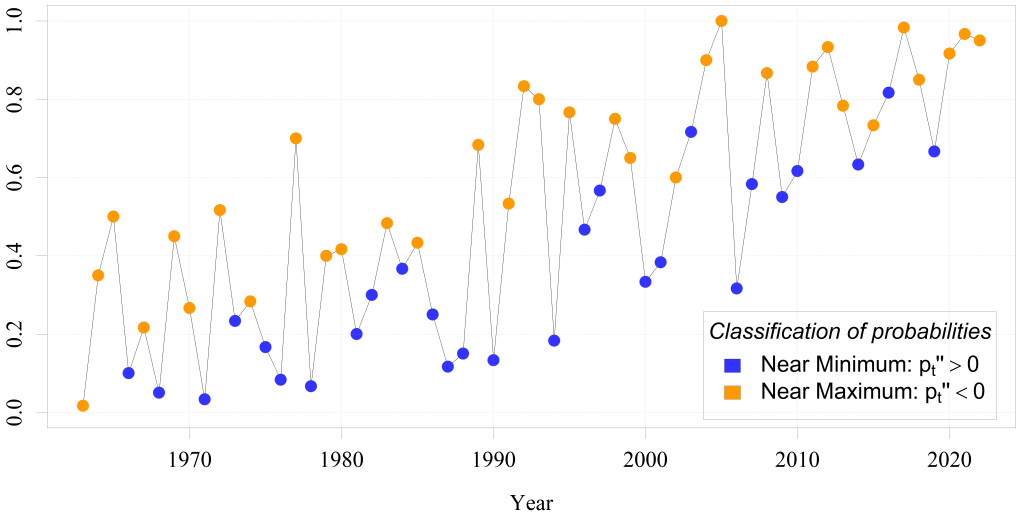

Figure 2.3: Cumulative probabilities for the estimated aggregate total losses.

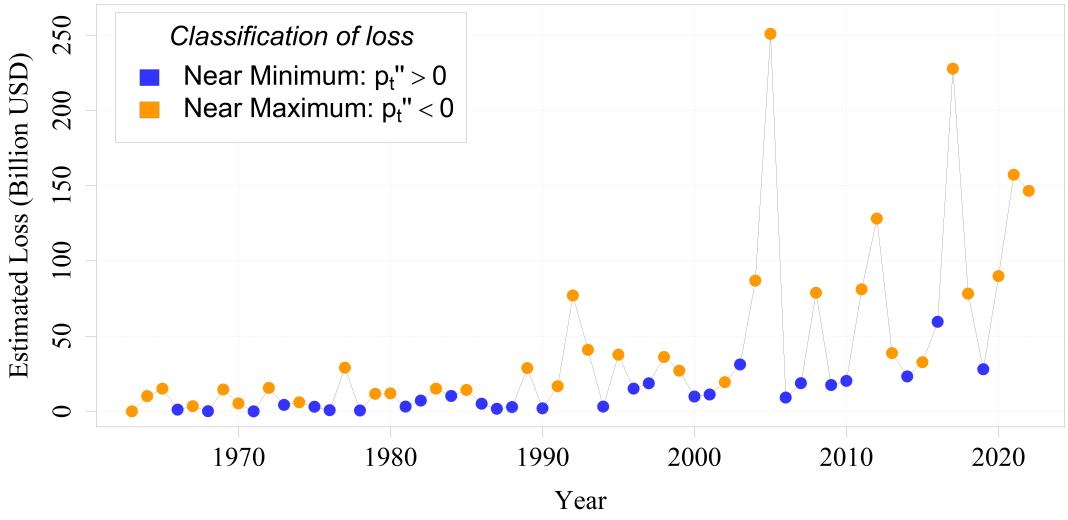

Figure 2.4: Classification of losses using the second-order difference of the cumulative probability values.

2.4 Loss Layers

Now that we have determined the the near maximum and minimum losses, we construct a regression model to approximate the expected values of near maximum and minimum losses, given a year. Consider the following regression models

$$\log(\boldsymbol{x}^{Nmin}) = \beta^{Nmin}\boldsymbol{y}^{Nmin} + \epsilon \tag{2.4.0.1}$$

and

$$\log(\boldsymbol{x}^{Nmax}) = \beta^{Nmax}\boldsymbol{y}^{Nmax} + \epsilon \tag{2.4.0.2}$$

where $\boldsymbol{y}^{Nmax}$ and $\boldsymbol{y}^{Nmin}$ are the corresponding years for the near maximum and near minimum loss values. We then use these coefficients to construct log-transformed linear regression as $\boldsymbol{y}$ as the independent variable and $log(\boldsymbol{x})$ and the target. We will get the two following functions.

$$\widehat{\log(\boldsymbol{x})} = \beta^{Nmin}\boldsymbol{y} \tag{2.4.0.3}$$

and

$$\widehat{\log(\boldsymbol{x})} = \beta^{Nmax}\boldsymbol{y} \tag{2.4.0.4}$$

Note that the $\widehat{\boldsymbol{x}_{LM}}$ represents the expected value of the low-medium, and $\widehat{\boldsymbol{x}_{MH}}$ represents the medium-high losses, given a year. Thereforem to set up each layer, we use these expected values. That is,

$$LM \text{ Layer} = \widehat{\log(\boldsymbol{x})} = \beta^{Nmin}\boldsymbol{y} \tag{2.4.0.5}$$

$$MH \text{ Layer} = \widehat{\log(\boldsymbol{x})} = \beta^{Nmax}\boldsymbol{y} \tag{2.4.0.6}$$

where $n = 60$ is the number of years, LM stands for low-medium losses and MH stands for medium-high losses. Please refer to appendix A.2 for the algorithm of the classification of loss and the loss layering.

Chapter 3

Results and Discussion

3.1 Results

3.1.1 Loss Classification

The classification of losses in the North and Central America region, utilizing the second-order difference method, has provided significant insights into the repercussions of natural disasters spanning over years.

Figures 2.2 and 2.4 depict the classified losses, using both approach of classifying by second-order difference of the losses observed over time and the cumulative probabilities in the North America region, wherein notable events such as Hurricane Andrew in 1992, Hurricane Ivan in 2004, Hurricane Katrina, Hurricane Wilma and wildfires in 2005, severe flooding in 2006, and wildfires in 2021 have had a considerable impact.

Notably, in Figure 2.2, the aggregated losses for these years have been classified as near maximum losses due to their considerable financial toll and significant impact on human lives, as we discueesed in Section 2.1. Figure 2.4 presents the alternative approach to loss classification, utilizing the loss space for the second-order difference. This method exhibits variations in the classification of losses. The main reason for this behavior is that the ECDF is a non-linear transformation of loss values. Therefore, the increment and decrements between two consecutive losses do not decrease or increase proportionally when transformed into cumulative probabilities. This non-linear transformation will lead to disparities in the concave and convex segments and subsequently affect the classification of losses. Utilizing cumulative probability offers a scaled approach, placing losses on a standardized range between 0 and 1 before assessing the curvature

of segments and classification, providing a clearer view of the underlying changes. However, this approach may overlook certain subtleties and extreme events linked to outliers in the data. Conversely, employing loss space captures the impact of rare and extreme events, which can result in a more conservative classification of losses.

For example, during the period encompassing 2004 and leading into 2005, the region under study faced a series of unprecedented meteorological events, giving rise to considerable fluctuations in loss values. The quick increase of losses during these events influenced the overall convexity and concavity of the cumulative probability function and loss values, leading to significant shifts and alterations in the loss classification. Figure 2.3 reveals that the shift in cumulative probability between 2004 and 2005 is not substantial, with 2005 exhibiting the lowest cumulative probability (indicating the least likelihood of occurrence or occurrence of the most significant loss), leading to a concave segment in the cumulative probability function, and consequently, a classification near the maximum loss. However, the actual losses during this period undergo drastic changes. Specifically, the loss in 2004 is considerably smaller than in 2005 and closer to the loss observed in 2003, resulting in a classification near the minimum loss.

3.1.2 Loss Layers

Figures 3.1 and 3.2 provide visual insights into the regression-derived near minimum and near maximum loss layers spanning from 1963 to 2022. Within this framework, each best-fit line signifies the anticipated average value of categorized loss values for specific years for the near minimum or maximum classified loss values. The attachment and exhaustion thresholds, separate distinct zones of loss classification. Losses beneath the attachment threshold signify a low-medium layer, where the reimbursement responsibility is for the original insurer. Between the attachment and exhaustion thresholds lies the medium-high loss layer, shifting insured payouts responsibility to the secondary insurer, assuming the original insurer's risk. Exceeding the exhaustion threshold places the liability on the original insurer once more, potentially straining their finances, and may lead to bankruptcy of the original insurer.

Furthermore, in Figures 3.1 and 3.2, whether losses classified by actual loss values or cumulative probabilities highlight a clear exponential growth pattern in both attachment and exhaustion thresholds, indicating a significant and concerning trajectory marked by escalating losses attributed to climate-induced disasters. This noticeable trend is further corroborated by the systematic classification of these losses, emphasizing the severity of climate-related risks as they progressively amplify over time. This dual approach, combining mathematical analysis with a structured categorization framework, offers a robust perspective on the increasingly urgent and intensifying challenges posed by the evolving climatic and weather conditions.

Climate change in North America has instigated significant shifts in weather patterns, leading to more frequent and severe extreme weather events such as hurricanes, wildfires, floods, and heatwaves [47]. This exponential increase in climate losses can be partially attributed to the amplification of feedback loops resulting from climate-induced shifts and heightened atmospheric and sea temperatures. For example, rising temperatures accelerate polar ice and glacier melt, culminating in elevated sea levels. These rising sea levels translate to floods and storm surges, particularly impacting coastal cities and precipitating substantial economic losses and property damage [18][34]. Additionally, ocean warming contributes to the energy and intensity of hurricanes, intensifying their landfall effects [61][35]. Prolonged heatwaves and droughts, exacerbated by climate change, heighten the probability and severity of wildfires, resulting in extensive property destruction and ecosystem degradation [36]. These interconnected feedback loops, the increase of the atmosphere and ocean surface, and anthropogenic green house gas effect, create a self-perpetuating cycle of climate-related disasters, contributing to the exponential rise in average losses.

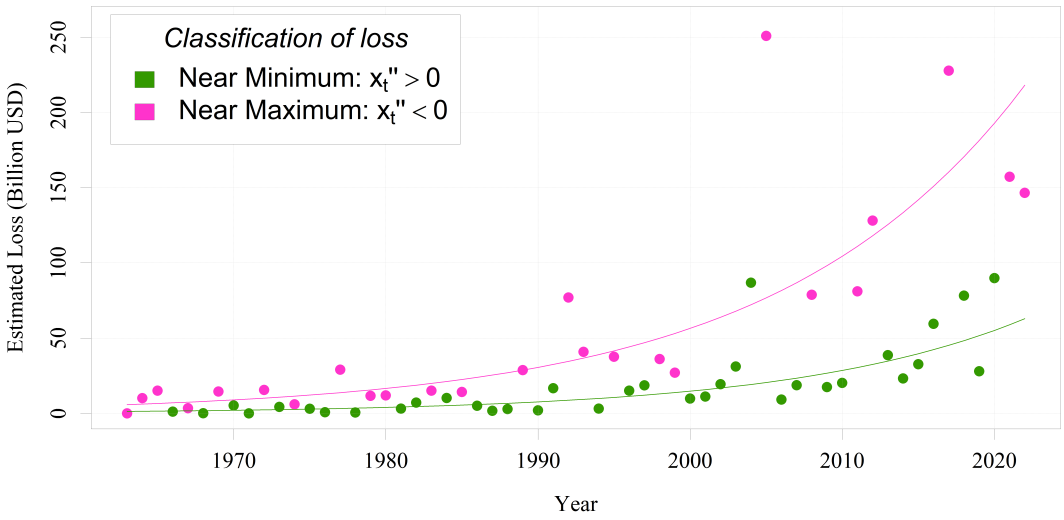

Figure 3.1: Attachment (green) and exhaustion (magenta) thresholds for classified losses using the second-order difference of the actual losses per year.

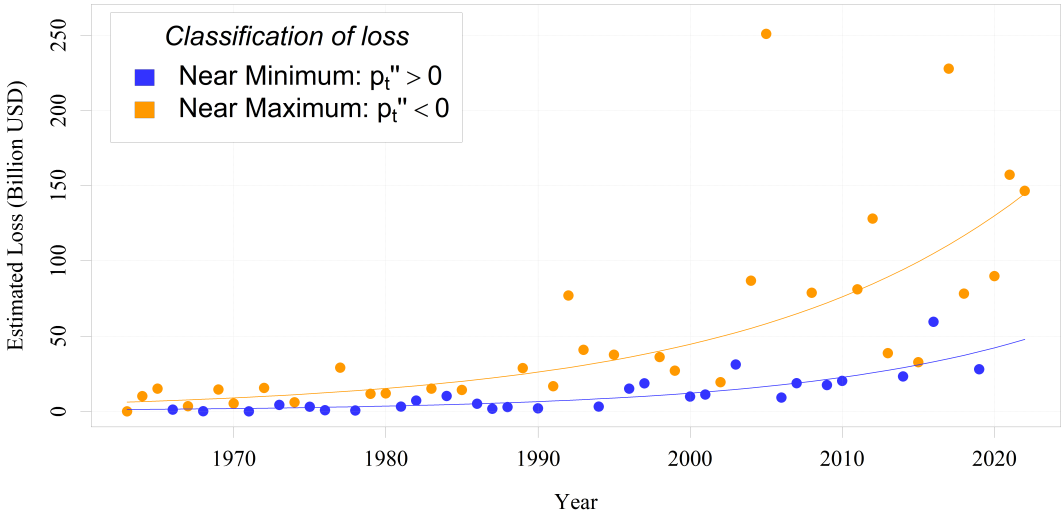

Figure 3.2: Attachment (blue) and exhaustion (orange) thresholds for classified losses using the second-order difference of the cumulative probabilities per year.

3.2 Discussion

The analysis begins by examining Figures 3.1 and 3.2, which illustrate a noteworthy observation regarding the attachment threshold. It is evident that when employing the probability space for loss classification, the attachment threshold is notably lower than when using the loss space. This intriguing finding holds the potential for both advantageous and disadvantageous implications. On the one hand, the lower attachment threshold signifies an increased reliance on reinsurers and innovative risk transfer mechanisms. These entities serve as a critical safety net by absorbing a portion of the insurer's risk, thereby safeguarding the insurer from the potential insolvency risk associated with significant catastrophic losses. Moreover, reducing reserves due to low attachment thresholds allows insurers to allocate more capital, enabling them to unlock resources for business expansion, product development, or other growth initiatives. However, this heightened dependence on external mechanisms comes with inherent costs, including reinsurance premiums, fees, and potential complexities tied to innovative risk transfer methods. These factors can impact an insurer's profitability and financial stability, warranting a comprehensive evaluation of the trade-offs involved.

Nevertheless, a pivotal question persists: How does the methodology employ a logarithmic transformation of losses before the threshold construction process? Addressing this inquiry, our approach involves utilizing various regression models designed to shape this crucial facet of the methodology. For a comprehensive analysis, we focus on Tables 3.1 and 3.2, where an intricate evaluation unfolds, meticulously comparing models across both the attachment and exhaustion thresholds. Each model undergoes scrutiny based on key metrics such as r^2, p-value, AIC, and BIC. Specifically, Table 3.1 presents models derived from losses classified by their actual values, while Table 3.2 showcases models constructed using cumulative probability values.

In Table 3.1, among the models for the attachment threshold, it is evident that the log-transform ($\log(\text{loss}) = -129 + 0.0659\,\text{year}$) exhibits the highest coefficient of determination ($r^2 = 0.750$) and the smallest p-value (1.87×10^{-11}), indicating a robust fit and vital statistical significance. Furthermore, this model possesses the lowest AIC (71.6) and BIC (76.3) values, implying a superior balance between goodness of fit and model complexity. Thus, the log-transform appears to be the most favorable choice for the attachment threshold, effectively capturing the underlying relationship between the loss and year variables. Similarly for the exhaustion threshold, the model with log-transform ($\log(\text{loss}) = -119 + 0.0614\,\text{year}$) is also a preferred, as this model achieves a significant ($r^2 = 0.772$) and a relatively small p-value (7.53×10^{-9}), underscoring its strong predictive capability and statistical significance. Furthermore, the associated AIC (52.4) and BIC (56.0) values are comparatively lower than those of other models. From Table 3.2, we notice that for the model that best defines the attachment threshold is the log-transform ($\log(\text{loss}) = -122 + 0.0624\,\text{year}$) exhibits the highest coefficient of determination ($r^2 = 0.759$),

the smallest p-value (3.36×10^{-9}), and lowest AIC (49.1) and BIC (52.9) values. The model that best the exhaustion threshold in Table 3.2 is also the log-transform model which provides superior balance between fit quality and model complexity. Figures 3.3, 3.4, 3.5, and 3.6 show the different constructed models in these two tables, and show cases the superiority of capturing the expected value of the two classified losses.

It becomes evident that, for both thresholds, the model employing a logarithmic transformation of loss values shows superior goodness of fit and significance compared to the alternative models. This tendency to effectively capture the relationship between loss and year variables, and the actuality that climate and weather-related disaster have been exponentially [31][26][53], highlights the rationale behind choosing the logarithmic transformation as the optimal approach. As a result, the methodology adopts this model for tracing attachment and exhaustion thresholds.

Regression Model	r^2	p-value	AIC	BIC
Attachment Threshold				
loss = $-2035 + 1.03$ year	0.489	2.93×10^{-6}	304	309
loss = $117000 - 118$ year $+ 0.03$ year^2	0.574	1.17×10^{-6}	300	306
loss = $-5459000 + 8273$ year $- 4.18$ year$^2 + 0.0007$ year^3	0.538	4.52×10^{-6}	301	309
log (loss) = $-129 + 0.0659$ year	0.750	1.87×10^{-11}	71.6	76.3
loss$^{0.5}$ = $-494 + 0.2502$ year	0.680	1.11×10^{-9}	177	182
loss$^{-0.5}$ = $-93.1 + 0.0472$ year	0.348	1.92×10^{-4}	109	113
Exhaustion Threshold				
loss = $-5798 + 2.94$ year	0.614	3.56×10^{-6}	265	268
loss = $205900 - 210$ year $+ 0.05$ year^2	0.669	5.27×10^{-6}	263	268
loss = $11870000 - 17780$ year $+ 8.88$ year$^2 - 0.0015$ year^3	0.678	2.14×10^{-5}	264	270
log (loss) = $-119 + 0.0614$ year	0.772	7.53×10^{-9}	52.4	56.0
loss$^{0.5}$ = $-765 + 0.3900$ year	0.763	1.18×10^{-8}	146	150
loss$^{-0.5}$ = $-27.6 + 0.0146$ year	0.488	1.02×10^{-4}	123	160

Table 3.1: Comparison of regression models for thresholds (**classified by aggregated total loss values**): linear, quadratic, and cubic polynomial powers, and log transformation, square root transformation, and inverse square root transformation of the loss target variable.

Regression Model	r^2	p-value	AIC	BIC
Attachment Threshold				
loss = $-1285 + 0.651$ year	0.589	2.95×10^{-6}	197	201
loss = $66650 - 67.6$ year $+ 1.712$ year^2	0.671	1.59×10^{-6}	193	198
loss = $-1985000 + 3022$ year $- 1.53$ year$^2 + 0.0003$ year^3	0.675	7.96×10^{-6}	194	201
log (loss) = $-122 + 0.0624$ year	0.759	3.36×10^{-9}	49.1	52.9
loss$^{0.5}$ = $-403 - 0.2040$ year	0.743	7.59×10^{-9}	115	119
loss$^{-0.5}$ = $-109 + 0.0552$ year	0.353	1.09×10^{-3}	190	194
Exhaustion Threshold				
loss = $-4454 + 2.26$ year	0.468	1.14×10^{-5}	351	356
loss = $132500 - 135$ year $+ 0.0345$ year^2	0.494	3.60×10^{-5}	352	358
loss = $5472000 - 8174$ year $+ 4.07$ year$^2 - 0.0007$ year^3	0.497	1.52×10^{-4}	354	361
log (loss) = $-103 + 0.0535$ year	0.706	9.67×10^{-10}	71.2	75.7
loss$^{0.5}$ = $-629 + 0.3209$ year	0.640	2.33×10^{-8}	199	204
loss$^{-0.5}$ = $-24.8 + 0.0132$ year	0.501	4.11×10^{-6}	76.3	121

Table 3.2: Comparison of regression models for thresholds (**classified by probability space**): linear, quadratic, and cubic polynomial powers, and log transformation, square root transformation, and inverse square root transformation.

(i) (A) Linear thresholds. (B) Quadratic thresholds.

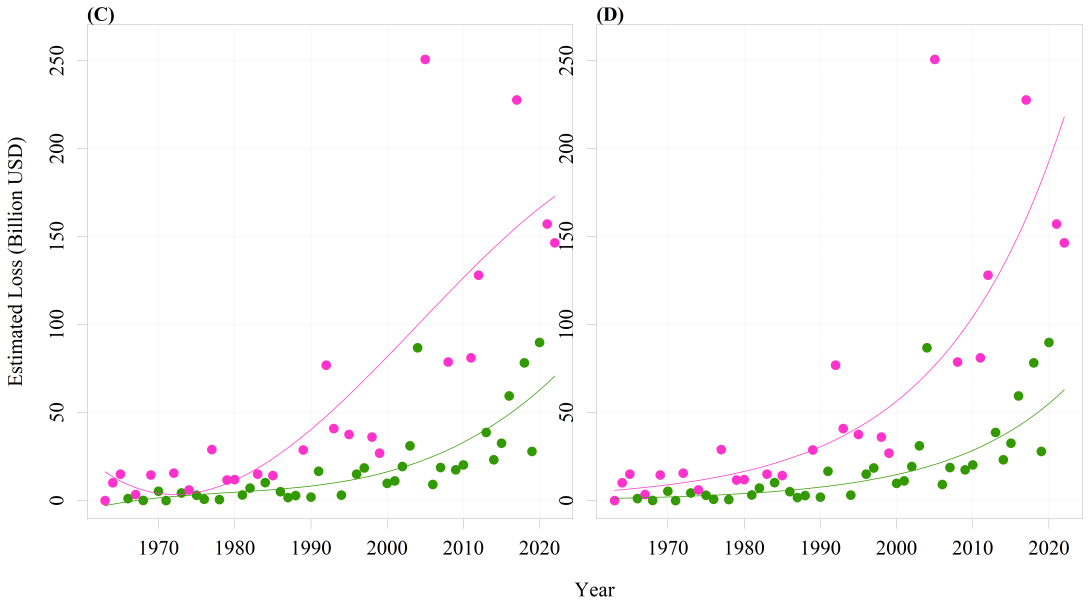

(ii) (C) Cubic thresholds. (D) Non-linear thresholds using log-transform of loss.

Figure 3.3: Different regression models for setting attachment (green) and exhaustion (magenta) thresholds for losses **classified by aggregated total loss values**.

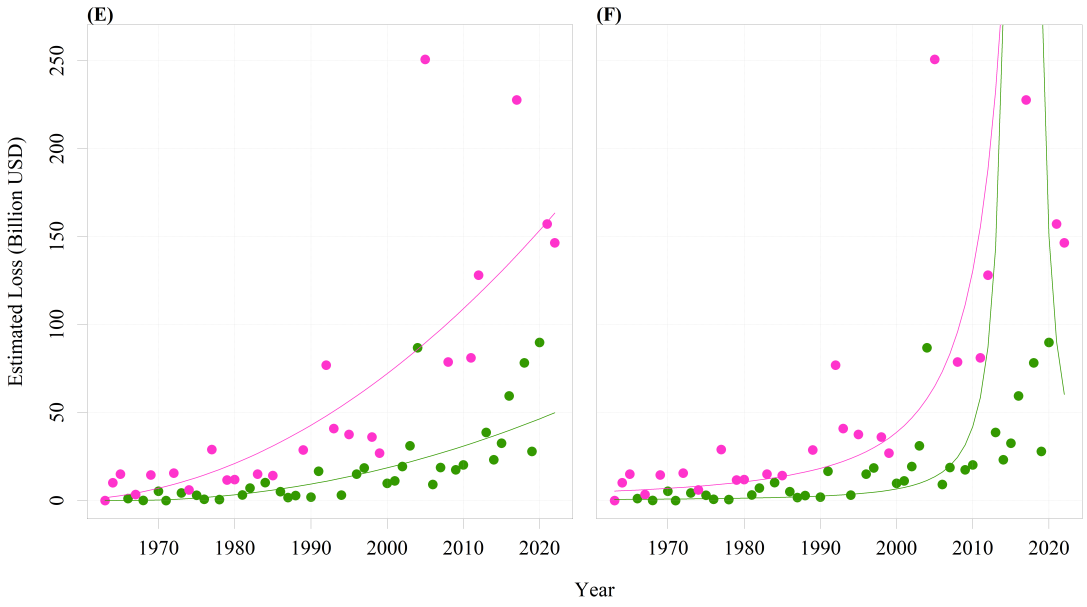

(i) (E) Non-linear thresholds using square root transformation of loss. (F) Non-linear thresholds using inverse square root transformation of loss.

Figure 3.4: Different regression models for setting attachment (green) and exhaustion (magenta) thresholds for losses **classified by aggregated total loss values**.

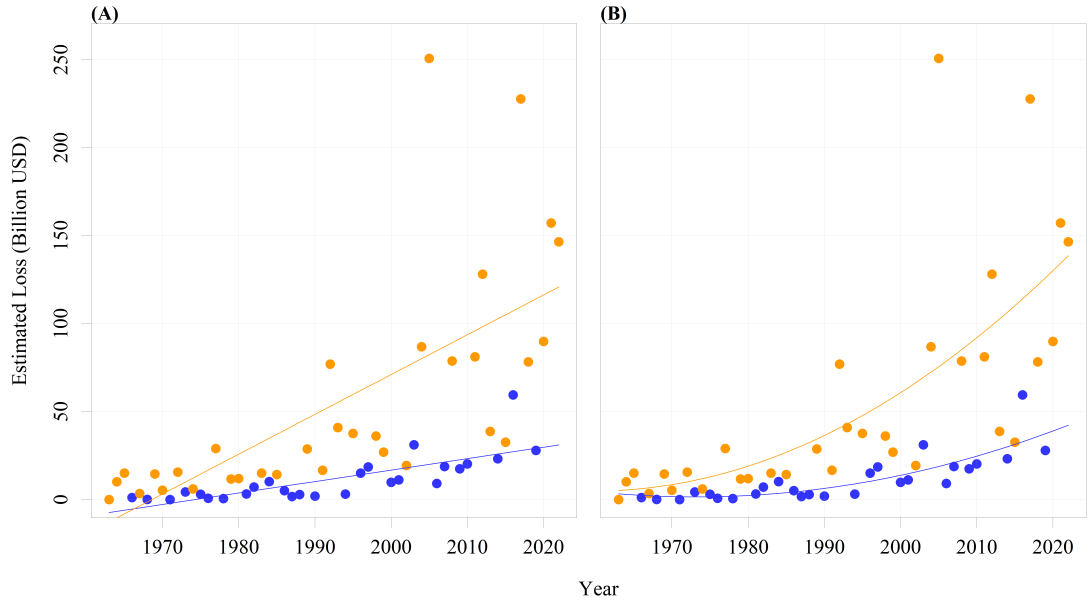

(i) (A) Linear thresholds. (B) Quadratic thresholds.

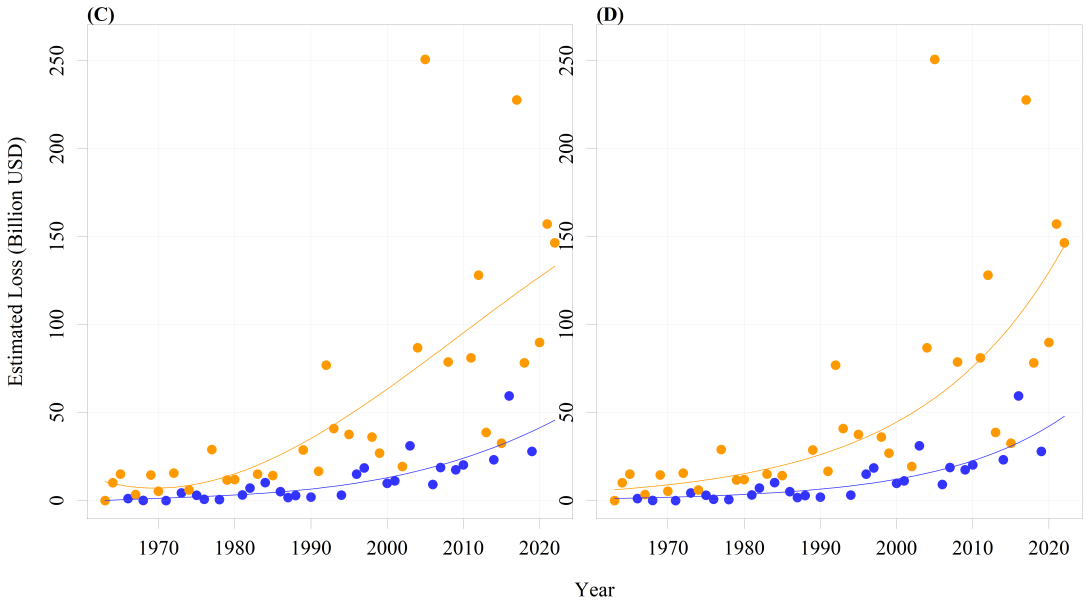

(ii) (C) Cubic thresholds. (D) Non-linear thresholds using log-transform of loss.

Figure 3.5: Different regression models for setting attachment (blue) and exhaustion (orange) thresholds for losses **classified by cumulative probability values**.

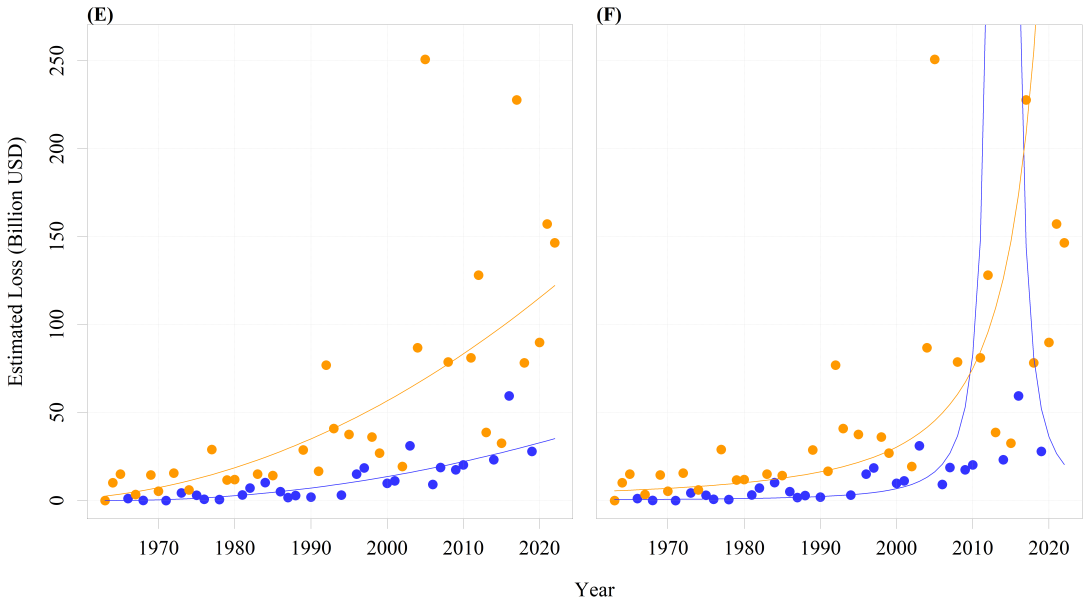

(i) (E) Non-linear thresholds using square root transformation of loss. (F) Non-linear thresholds using inverse square root transformation of loss.

Figure 3.6: Different regression models for setting attachment (blue) and exhaustion (orange) thresholds for losses **classified by cumulative probability values**.

3.3 Conclusion

This project has introduced a methodical approach to classify losses based on their magnitudes, culminating in a unambiguous categorization scheme. As we saw in section 3.1, that the classification of loss correctly categorized losses in years that extreme disasters had affected the North America region. Furthermore, the classification of losses through the second-order difference method, coupled with observing an exponential surge in the two classified loss categories, holds essential significance in comprehending the amplification of climate catastrophes. This empirical evidence underscores the fast increase of losses linked to climate-related events and emphasizes the necessity of adaptive policies for (re)insurers to mitigate the impact of increasing losses. The simplicity of this model is an accomplishment, as the model does not require a granular analysis of a range of factors, such as property damage and casualties, which significantly reduces the complexity of the classification model, and provides a simple, but helpful model for the insurer and policymaker.

Furthermore, our research has forged a resilient framework for allocating loss layers, effectively determining attachment and exhaustion thresholds. The effectiveness and robustness of this framework stem from a rigorous exploration of diverse regression models in section 3.2, culminating in the identification of a model that not only demonstrated the highest level of statistical significance but also conformed seamlessly with the prevailing literature concerning climate and weather-related disasters. The careful selection of this model, aligned with established research paradigms, further highlights the usefulness of this approach for an insurer.

By successfully classifying losses and constructing loss layers, an insurer can use this model as a helpful tool to increase their coverage for the policyholders for climate and weather-related disasters.

Moving forward, several promising avenues for future research emerge from our current findings, offering opportunities to enrich and expand upon the established framework. An interesting possibility lies in extending our model to encompass diverse geographical regions. Exploring how our methodology performs across different locales, each characterized by unique climatic dynamics, can provide valuable insights into our approach's broader applicability and robustness. However, this possibility heavily relies on the availability of estimated loss data for regions other than North America. A further refinement of our model is to address specific meteorological, climatological, and hydrological events presents an exciting avenue. So far, we have used the aggregated loss over these events. By tailoring the framework to individual event types, we can reveal patterns and relationships that may not be evident in a broader context, thus enhancing our methodology's predictive power. Furthermore, incorporating additional features into our regression model holds promise for a more comprehensive understanding of loss

allocation dynamics. Variables such as the frequency of disasters and the number of affected people in the region can contribute to a model that captures a wider spectrum of influences, potentially bolstering the prediction of the thresholds' accuracy. A logical progression involves extending our model to embrace a probabilistic paradigm for each loss layer, such as a Markov chain, which will help the insurer to construct long-term transitional probabilities for losses within each loss layer.

These avenues of future work enhance the depth of our methodology and inform more effective disaster risk management strategies, thereby contributing to a more resilient and prepared future in the face of evolving climatic challenges.

References

[1] Jeroen C J H Aerts and W J Wouter Botzen. Climate change impacts on pricing long-term flood insurance: A comprehensive study for the netherlands. *Global Environmental Change*, 21(3):1045–1060, 2011.

[2] Butch Bacani, Nick Robins, and Jeremy McDaniels. Harnessing insurance for sustainable development. Technical report, 2015. Available at: https://www.unepfi.org/psi/wp-content/uploads/2015/06/Insurance2030.pdf.

[3] Oscar Becerra, Eduardo Cavallo, and Ilan Noy. Foreign aid in the aftermath of large natural disasters: Aid after disasters. *Review of Development Economics*, 18(3):445–460, 2014.

[4] Corina Birghila, Georg Ch Pflug, and Stefan Hochrainer-Stigler. Risk-layering and optimal insurance uptake under ambiguity: With an application to farmers exposed to drought risk in austria. *Risk Analysis: An Official Publication of the Society for Risk Analysis*, 42(12):2639–2655, 2022.

[5] Günter Blöschl, Julia Hall, Alberto Viglione, Rui A P Perdigão, Juraj Parajka, Bruno Merz, David Lun, Berit Arheimer, Giuseppe T Aronica, Ardian Bilibashi, Miloň Boháč, Ognjen Bonacci, Marco Borga, Ivan Čanjevac, Attilio Castellarin, Giovanni B Chirico, Pierluigi Claps, Natalia Frolova, Daniele Ganora, Liudmyla Gorbachova, Ali Gül, Jamie Hannaford, Shaun Harrigan, Maria Kireeva, Andrea Kiss, Thomas R Kjeldsen, Silvia Kohnová, Jarkko J Koskela, Ondrej Ledvinka, Neil Macdonald, Maria Mavrova-Guirguinova, Luis Mediero, Ralf Merz, Peter Molnar, Alberto Montanari, Conor Murphy, Marzena Osuch, Valeryia Ovcharuk, Ivan Radevski, José L Salinas, Eric Sauquet, Mojca Šraj, Jan Szolgay, Elena Volpi, Donna Wilson, Klodian Zaimi, and Nenad Živković. Changing climate both increases and decreases european river floods. *Nature*, 573(7772):108–111, 2019.

[6] Maya K Buchanan, Scott Kulp, Lara Cushing, Rachel Morello-Frosch, Todd Nedwick, and Benjamin Strauss. Sea level rise and coastal flooding threaten affordable housing. *Environmental Research Letters*, 15(12):124020, 2020.

[7] H Jithamala Caldera and S C Wirasinghe. A universal severity classification for natural disasters. *Natural Hazards (Dordrecht, Netherlands)*, 111(2):1533–1573, 2022.

[8] Miguel A Centeno, Manish Nag, Thayer S Patterson, Andrew Shaver, and A Jason Windawi. The emergence of global systemic risk. *Annual Review of Sociology*, 41(1):65–85, 2015.

[9] Rachel J C Chen. Effects of climate change in north america: An overview. *Journal of Sustainable Development*, 4(3), 2011.

[10] Ben Clarke, Friederike Otto, Rupert Stuart-Smith, and Luke Harrington. Extreme weather impacts of climate change: an attribution perspective. *Environmental Research: Climate*, 1(1):012001, 2022.

[11] Christophe Courbage and Maryam Golnaraghi. Extreme events, climate risks and insurance. *The Geneva Papers on Risk and Insurance Issues and Practice*, 47(1):1–4, 2022.

[12] Crawford & Company. Hurricane wilma october 15-25, 2005 situation and response paper. Technical report, 2005. Available at: https://assets.crawfordandcompany.com/media/182925/hurricane_wilma_situation_paper.pdf.

[13] F Daniel, W Engert, D Maclean, and Department of Monetary and Financial Analysis. The bank of canada as lender of last resort. Technical report, 2005. Available at: https://www.bankofcanada.ca/wp-content/uploads/2010/06/daniel.pdf.

[14] Andrew L Dannenberg, Howard Frumkin, Jeremy J Hess, and Kristie L Ebi. Managed retreat as a strategy for climate change adaptation in small communities: public health implications. *Climatic Change*, 153(1-2):1–14, 2019.

[15] Charles Doktycz and Mark Abkowitz. Loss and damage estimation for extreme weather events: State of the practice. *Sustainability*, 11(15):4243, 2019.

[16] J Douris, Geunhye Kim, and World Meteorological Organization. WMO atlas of mortality and economic losses from weather, climate and water extremes (1970–2019) (WMO-No. 1267). Technical report, 2021. Available at: https://library.wmo.int/doc_num.php?explnum_id=10989.

[17] EM-DAT. Em-dat: The international disaster database, 2008. Available at: https://www.emdat.be/.

[18] Eugénie S Euskirchen, Eban S Goodstein, and Henry P Huntington. An estimated cost of lost climate regulation services caused by thawing of the arctic cryosphere. *Ecological Applications: A Publication of the Ecological Society of America*, 23(8):1869–1880, 2013.

[19] Federal Emergency Management Agency. *National Flood Insurance Program: Flood Insurance Manual*, 2022. Available at: https://www.fema.gov/sites/default/files/documents/fema_nfip-flood-insurance-full-manual_102022.pdf.

[20] S Hall, B Evarts, and National Fire Protection Association. Fire loss in the united states during 2021. Technical report, 2022. Available at: https://www.nfpa.org/~/media/Files/News%20and%20Research/Fire%20statistics%20and%20reports/US%20Fire%20Problem/osFireLoss.ashx.

[21] Stefan Hochrainer-Stigler and Karina Reiter. Risk-layering for indirect effects. *International Journal of Disaster Risk Science*, 12(5):770–778, 2021.

[22] Gareth James, Daniela Witten, Trevor Hastie, and Robert Tibshirani. *An introduction to statistical learning: With applications in R*. Springer, New York, NY, 2 edition, 2022.

[23] P Jarzabkowski, K Chalkias, D Clarke, E Iyahen, D Stadtmueller, and A Zwick. Insurance for climate adaptation: Opportunities and limitations. *Rotterdam and Washington, DC*, 2019.

[24] Tom Johnston and Canadian Interagency Forest Fire Centre. Canada report 2005. Technical report, 2005. Available at: https://gfmc.online/wp-content/uploads/2005-Canada-Report.pdf.

[25] Rebecca Louise Jones, Debarati Guha-Sapir, and Sandy Tubeuf. Human and economic impacts of natural disasters: can we trust the global data? *Scientific Data*, 9(1):572, 2022.

[26] Thomas R Karl and David R Easterling. Climate extremes: Selected review and future research directions. In *Weather and Climate Extremes*, pages 309–325. Springer Netherlands, Dordrecht, 1999.

[27] Razmig Keucheyan. Insuring climate change: New risks and the financialization of nature: Debate: Insuring climate change. *Development and Change*, 49(2):484–501, 2018.

[28] Rawle O King and CRS Report for Congress. Hurricane katrina: Insurance losses and national capacities for financing disaster risk. Technical report, 2005. Available at: https://www.everycrsreport.com/files/20050915_RL33086_ad330b1de024dd62d0ddb79f0b93fc69601437e0.pdf.

[29] Richard D Knabb, Jamie R Rhome, Daniel P Brown, National Hurricane Center, National Oceanic and Atmospheric Administration, and National Flood Insurance Program. Tropical cyclone report hurricane katrina 23-30 august 2005. Technical report, 2023. Available at: https://www.nhc.noaa.gov/data/tcr/AL122005_Katrina.pdf.

[30] Kati Kraehnert, Daniel Osberghaus, Christian Hott, Lemlem Teklegiorgis Habtemariam, Frank Wätzold, Lutz Philip Hecker, and Svenja Fluhrer. Insurance against extreme weather events: An overview. *Review of Economics.*, 72(2):71–95, 2021.

[31] Howard Kunreuther. Risk management solutions for climate change-induced disasters. *Risk Analysis: An Official Publication of the Society for Risk Analysis*, 40(S1):2263–2271, 2020.

[32] Francesco Lamperti, Valentina Bosetti, Andrea Roventini, and Massimo Tavoni. The public costs of climate-induced financial instability. *Nature Climate Change*, 9(11):829–833, 2019.

[33] Davide Lanfranchi and Laura Grassi. Examining insurance companies' e of technology for innovation. *The Geneva Papers on Risk and Insurance Issues and Practice*, 47(3):520–537, 2022.

[34] Judy Lawrence, Paula Blackett, and Nicholas A Cradock-Henry. Cascading climate change impacts and implications. *Climate Risk Management*, 29(100234):100234, 2020.

[35] Emma L Levin and Hiroyuki Murakami. Impact of anthropogenic climate change on united states major hurricane landfall frequency. *Journal of Marine Science and Engineering*, 7(5):135, 2019.

[36] Yan Li, Kaiyu Guan, Gary D Schnitkey, Evan DeLucia, and Bin Peng. Excessive rainfall leads to maize yield loss of a comparable magnitude to extreme drought in the united states. *Global Change Biology*, 25(7):2325–2337, 2019.

[37] Joanne Linnerooth-Bayer and Stefan Hochrainer-Stigler. Financial instruments for disaster risk management and climate change adaptation. *Climatic Change*, 133(1):85–100, 2015.

[38] Vyacheslav Lyubchich, Nathaniel K Newlands, Azar Ghahari, Tahir Mahdi, and Yulia R Gel. Insurance risk assessment in the face of climate change: Integrating data science and statistics. *Wiley Interdisciplinary Reviews. Computational Statistics*, 11(4):e1462, 2019.

[39] Sheikh Mansoor, Iqra Farooq, M Mubashir Kachroo, Alaa El Din Mahmoud, Manal Fawzy, Simona Mariana Popescu, M N Alyemeni, Christian Sonne, Jorg Rinklebe, and Parvaiz Ahmad. Elevation in wildfire frequencies with respect to the climate change. *Journal of Environmental Management*, 301(113769):113769, 2022.

[40] Reinhard Mechler, Laurens M Bouwer, Joanne Linnerooth-Bayer, Stefan Hochrainer-Stigler, Jeroen C J H Aerts, Swenja Surminski, and Keith Williges. Managing unnatural disaster risk from climate extremes. *Nat. Clim. Chang.*, 4(4):235–237, 2014.

[41] Ash Morgan. The impact of hurricane ivan on expected flood losses, perceived flood risk, and property values. *Journal of Housing Research*, 16(1):47–60, 2007.

[42] Ali Nejat, Laura Solitare, Edward Pettitt, and Hamed Mohsenian-Rad. Equitable community resilience: The case of winter storm uri in texas. *Int. J. Disaster Risk Reduct.*, 77(103070):103070, 2022.

[43] OECD. Disaster risk assessment and risk financing: A G20 / OECD METHODOLOGICAL FRAMEWORK. Technical report, 2016. Available at: https://www.oecd.org/gov/risk/G20disasterriskmanagement.pdf.

[44] Arlene Oetomo, Niloofar Jalali, Paula Dornhofer Paro Costa, and Plinio Pelegrini Morita. Indoor temperatures in the 2018 heat wave in quebec, canada: Exploratory study using ecobee smart thermostats. *JMIR Formative Research*, 6(5):e34104, 2022.

[45] Jonathan T Overpeck and Bradley Udall. Climate change and the aridification of north america. *Proceedings of the National Academy of Sciences of the United States of America*, 117(22):11856–11858, 2020.

[46] Tianze Pang, Xiuquan Wang, Rana Ali Nawaz, Genevieve Keefe, and Toyin Adekanmbi. Coastal erosion and climate change: A review on coastal-change process and modeling. *Ambio*, 2023.

[47] A. Patt, L. Rajamani, P. Bhandari, A. Ivanova Boncheva, A. Caparrós, K. Djemouai, I. Kubota, J. Peel, A.P. Sari, D.F. Sprinz, and J. Wettestad. International cooperation. In P.R. Shukla, J. Skea, R. Slade, A. Al Khourdajie, R. van Diemen, D. McCollum, M. Pathak, S. Some, P. Vyas, R. Fradera, M. Belkacemi, A. Hasija, G. Lisboa, S. Luz, and J. Malley, editors, *Climate Change 2022: Mitigation of Climate Change. Contribution of Working Group III to the Sixth Assessment Report of the Intergovernmental Panel on Climate Change*, book section 14. Cambridge University Press, Cambridge, UK and New York, NY, USA, 2022. Available at: https://www.ipcc.ch/report/ar6/wg3/downloads/report/IPCC_AR6_WGIII_Chapter14.pdf.

[48] Tarryn Phillips. The everyday politics of risk: Managing diabetes in fiji. *Medical Anthropology*, 39(8):735–750, 2020.

[49] Jennifer Reynolds. Gambling on big data: Designing risk in social casino games. *European Journal of Risk Regulation*, 10(1):116–131, 2019.

[50] Elisabeth L Rosvold and Halvard Buhaug. GDIS, a global dataset of geocoded disaster locations. *Scientific Data*, 8(1):61, 2021.

[51] Ridgway Scott. Interpolated boundary conditions in the finite element method. *SIAM Journal on Numerical Analysis*, 12(3):404–427, 1975.

[52] S K Smith and C McCarty. Demographic effects of natural disasters: a case study of hurricane andrew. *Demography*, 33(2):265–275, 1996.

[53] Manmohan S Sodhi. Natural disasters, the economy and population vulnerability as a vicious cycle with exogenous hazards. *Journal of Operations Management*, 45(1):101–113, 2016.

[54] Dan Stefanica. *A Primer For The Mathematics Of Financial Engineering*. Financial Engineering Press, first edition edition, April 2008.

[55] U.S. Department of Commerce, National Oceanic and Atmospheric Administration, and National Weather Service. Hurricane andrew: South florida and louisiana august 23-26, 1992. Technical report, 1993. Available at: https://www.weather.gov/media/publications/assessments/andrew.pdf.

[56] Erika Von Mutius and Hermelijn H Smits. Primary prevention of asthma: from risk and protective factors to targeted strategies for prevention. *Lancet*, 2020.

[57] Rafa l Walasek and Janusz Gajda. Fractional differentiation and its use in machine learning. *International Journal of Advances in Engineering Sciences and Applied Mathematics*, 13(2-3):270–277, 2021.

[58] Qingsong Wen, Jingkun Gao, Xiaomin Song, Liang Sun, and Jian Tan. RobustTrend: A huber loss with a combined first and second order difference regularization for time series trend filtering. 2019.

[59] R C Wilkinson, P K Clark, D H Craighead, J W Dean, A H Silverman, and M G White. Financial reinsurance. *Journal of the Institute of Actuaries*, 120(2):311–380, 1993.

[60] Suyang Yu and Lily Hsueh. Do wildfires exacerbate COVID-19 infections and deaths in vulnerable communities? evidence from california. *Journal of Environmental Management*, 328(116918):116918, 2023.

[61] Fan Zhang and Ming Li. Impacts of ocean warming, sea level rise, and coastline management on storm surge in a semienclosed bay. *Journal of Geophysical Research. Oceans*, 124(9):6498–6514, 2019.

[62] Yi-Jie Zhu, Jennifer M Collins, Philip J Klotzbach, and Carl J Schreck. Hurricane ida (2021): Rapid intensification followed by slow inland decay. *Bulletin of the American Meteorological Society*, 103(10):E2354–E2369, 2022.

APPENDICES

Appendix A

A.1 Difference Method Proofs

Central difference. We have a series of discrete values, $\{x_t\} = (x_t : t = 1, 2, ..., 60)$ at annual intervals of time. Consider 3 time indices, namely index $t-1$, t, and $t+1$, corresponding to *current* and *next* time indices. Since we have annual data points, then let $\Delta t = h = 1$ represent the loss intervals. Furthermore, let us use Newtonian notation for derivatives, namely, $x'_t, x''_t, ...$ The first-order difference scheme that follows from expanding the Taylor series at $t+1$ and $t-1$ according to

$$x_{t-1} = x_t - hx'_t + \frac{h^2}{2!}x''_t - \frac{h^3}{3!}x'''_t + O(h^4) \tag{A.1.0.1}$$

$$x_{t+1} = x_t + hx'_t + \frac{h^2}{2!}x''_t + \frac{h^3}{3!}x'''_t + O(h^4) \tag{A.1.0.2}$$

Using the appropriate differencing coefficients and subtracting the term A.1.0.1 from A.1.0.2 yields

$$x'_t = \frac{x_{t+1} - x_{t-1}}{h} + O(h^2) \tag{A.1.0.3}$$

By setting $h = 1$, then the first-order difference is estimated as

$$x'_t \approx \hat{x}'_t = x_{t+1} - x_{t-1} \tag{A.1.0.4}$$

By adding A.1.0.1 and A.1.0.2, without any coefficient adjustment, we can write the second-order difference scheme to approximate the second derivative of p_t as

$$x''_t = \frac{x_{t+1} - 2x_t + x_{t-1}}{h^2} + O(h^2) \tag{A.1.0.5}$$

By setting $h = 1$, then the second-order difference is estimated as

$$x_t'' \approx \hat{x}_t'' = x_{t+1} - 2x_t + x_{t-1} \tag{A.1.0.6}$$

□

Forward difference. Similarly, we have a series of discrete values, $\{x_t\} = (x_t : t = 1, 2, ..., 60)$ at annual intervals of time. Consider 3 time indices, namely index t, $t + 1$, and $t + 2$. The second-order difference scheme that gives the initial Neumann boundary condition follows from expanding the Taylor series at these time indeces according to

$$x_{t+1} = x_t + hx_t' + \frac{h^2}{2!}x_t'' + O(h^3) \tag{A.1.0.7}$$

$$x_{t+2} = x_t + (2h)x_t' + \frac{(2h)^2}{2!}x_t'' + O(h^3) \tag{A.1.0.8}$$

Using the appropriate differencing coefficients, we have

$$x_{t+1} = x_t - 2hx_t' + \frac{1}{2}h^2x_t'' + O(h^3) \tag{A.1.0.9}$$

$$x_{t+2} = x_t - 4hx_t' + 2h^2x_t''O(h^3) \tag{A.1.0.10}$$

Further, subtracting twice A.1.0.9 from A.1.0.10 will yield

$$x_t'' = \frac{x_{t+2} - 2x_{t+1} + x_t}{h^2} + O(h) \tag{A.1.0.11}$$

By setting $h = 1$, then the second-order difference is estimated as

$$x_t'' \approx x_t'' = x_{t+2} - 2x_{t+1} + x_t \tag{A.1.0.12}$$

□

Backward difference. We have a series of discrete values, $\{x_t\} = (x_t : t = 1, 2, ..., 60)$ at annual intervals of time. Consider 3 time indices, namely index $t - 2$, $t - 1$, and t. The second-order difference scheme that gives the final Neumann boundary condition follows from expanding the Taylor series at these time indeces according to

$$x_{t-1} = x_t - hx_t' + \frac{h^2}{2!}x_t'' + O(h^3) \tag{A.1.0.13}$$

$$x_{t-2} = x_t - (2h)x'_t + \frac{(2h)^2}{2!}x''_t + O(h^3) \tag{A.1.0.14}$$

Using the correct differencing coefficients, we have

$$x_{t-1} = x_t + 2hx'_t + \frac{1}{2}h^2x''_t + O(h^3) \tag{A.1.0.15}$$

$$x_{t-2} = x_t + 4hx'_t + 2h^2x''_tO(h^3) \tag{A.1.0.16}$$

Further, subtracting twice A.1.0.15 from A.1.0.16 will yield

$$x''_t = \frac{p_{t-2} - 2x_{t-1} + x_t}{h^2} + O(h) \tag{A.1.0.17}$$

By setting $h = 1$, then the second-order difference is estimated as

$$x''_t \approx x''_t = x_{t-2} - 2x_{t-1} + x_t \tag{A.1.0.18}$$

□

A.2 Algorithm for loss classification and loss layering

Algorithm 1 Second-order Difference Loss Classification Using Exceedance Probability Algorithm

Input: exceedance probability vector p with 60 elements, where $0 \leq p \leq 1$ and $h = 1$.
Set class 1 for near maximum and 2 for near minimum loss values.
for $t = 2$ to 59 **do**
    $a_t \leftarrow \frac{x_{t+1}-2x_t+x_{t-1}}{h^2}$
end for
$a_1 \leftarrow \frac{x_1-2x_2+x_3}{h^2}$ (initial Neumann boundary condition)
$a_{60} \leftarrow \frac{x_{58}-2x_{59}+x_{59}}{h^2}$ (final Neumann boundary condition)
for $t = 1$ to 60 **do**
    if $a_t < 0$ **then**
        $x_i^{Nmax} \leftarrow \hat{F}^{-}1(p_t)$
        $x_{[i,\text{class}]}^{new} \leftarrow (x_i^{Nmax}, 1)$ (near maximum loss values)
    else if $a_t > 0$ **then**
        $x_i^{Nmin} \leftarrow \hat{F}^{-}1(p_t)$
        $x_{[i,\text{class}]}^{new} \leftarrow (x_i^{Nmin}, 2)$ (near minimum loss values)
    end if
end for
return x^{new}

Algorithm 2 Near maximum and near minimum regression coefficients

Input: Data set $[\boldsymbol{y}, \boldsymbol{x}]$, where $\boldsymbol{x}$ is either near maximum or minimum loss values and $\boldsymbol{y}$ is the vector of years for the corresponding loss values
Input: Confidence level α
Compute log-transform of $\boldsymbol{x}$ as $\boldsymbol{z} = \ln \boldsymbol{x}$
Calculate coefficients using normal equations as $\beta = (\boldsymbol{z}\boldsymbol{z}^T)^{-1}\boldsymbol{z}^T\boldsymbol{y}$
return β

Algorithm 3 Near maximum and near minimum loss layers

Input: Data set $[\boldsymbol{y}, \boldsymbol{x}]$, where $\boldsymbol{x}$ is all the available losses and their corresponding years $\boldsymbol{y}$

Input: Confidence level α

Input: β^{Nmax} and $beta^{Nmin}$ coefficients

Compute log-transform of $\boldsymbol{x}$ as $\boldsymbol{z} = \ln \boldsymbol{x}$

Compute the predicted values: $\hat{\boldsymbol{z}}^{Nmax} = \beta^{Nmax}\boldsymbol{y}$

Compute the predicted values: $\hat{\boldsymbol{z}}^{Nmin} = \beta^{Nmin}\boldsymbol{y}$

return $\exp[\hat{\boldsymbol{z}}^{Nmax}]$ as LM loss layer and $\exp[\hat{\boldsymbol{z}}^{Nmin}]$ as MH loss layer